JOURNAL OF THERMOPHYSICS AND HEAT TRANSFER
Vol. 25, No. 1, January–March 2011

# Thermal Tomography Problem in Estimating the Unknown Interfacial Surface

Cheng-Hung Huang* and Chia-Ying Liu†
*National Cheng-Kung University, Tainan 701, Taiwan, Republic of China*

DOI: 10.2514/1.49401

**A thermal tomography problem, i.e., the shape identification problem or inverse geometry problem, in estimating the interfacial geometry for three-dimensional multiple region domains is examined in this study based on the conjugate gradient method (or the so-called iterative regularization method) and commercial code CFD-ACE+. The present work is classified as the function estimation in the thermal tomography calculation, since it is assumed that no prior information is available on the functional form of the unknown interfacial geometry. The accuracy of this thermal tomography analysis is examined using the simulated temperatures measured by an imaginary infrared scanner. Different temperature-measurement positions and errors are considered in the numerical experiments to justify the validity of the present algorithm in solving the three-dimensional thermal tomography problem. Finally, it is concluded that the reliable interfacial configurations can be estimated by the conjugate gradient method.**

## Nomenclature

| | | |
|---|---|---|
| $h$ | = | heat transfer coefficient |
| $J$ | = | functional defined by Eq. (4) |
| $J'$ | = | gradient of functional defined by Eq. (21) |
| $k$ | = | thermal conductivity |
| $M$ | = | the total number of extracting points for the measured temperatures |
| $n$ | = | the outward normal unit vector |
| $P(x, y)$ | = | direction of descent defined by Eq. (6) |
| $T(x, y, z)$ | = | estimated temperature |
| $Y$ | = | measured temperature |
| $\beta$ | = | search step size |
| $\Gamma(x, y)$ | = | unknown irregular interfacial configuration |
| $\gamma$ | = | conjugate coefficient |
| $\Delta$ | = | perturbed value |
| $\Delta T(x, y, z)$ | = | sensitivity function defined by Eqs. (8) and (9) |
| $\delta(\bullet)$ | = | Dirac delta function |
| $\varepsilon$ | = | convergence criterion |
| $\lambda(x, y, z)$ | = | Lagrange multiplier defined by Eqs. (17) and (18) |
| $\sigma$ | = | standard deviation of the measurement error |
| $\Omega$ | = | computational domain |
| $\omega$ | = | random number |

*Superscript*

| | | |
|---|---|---|
| $n$ | = | iteration index |

*Subscripts*

| | | |
|---|---|---|
| 1 | = | region 1 |
| 2 | = | region 2 |

Received 17 February 2010; revision received 8 August 2010; accepted for publication 15 August 2010. 

*Professor, Department of Systems and Naval Mechatronic Engineering; chhuang@mail.ncku.edu.tw (Corresponding Author).

†Graduate Student, Department of Systems and Naval Mechatronic Engineering.

## I. Introduction

THE applications of inverse heat conduction problems can be found in several engineering fields to estimate the unknown thermal quantities, such as the determination of unknown thermal properties [1], heat fluxes [2] and heat sources [3], etc., when the geometry of the physical problem under consideration is known.

However, when the geometry of the problems is unknown and to be estimated, the techniques of thermal tomography problem, i.e., the shape identification problem or inverse geometry problem, should be used to estimate the unknown domain configurations. For the thermal tomography problem, due to its inherent nature, it requires a complete regeneration of the mesh as the geometry evolves. Moreover, the continuous evolution of the geometry itself poses certain difficulties in arriving at analytical or numerical solutions. For this reason it is necessary to use an efficient technique to handle the problems with irregular surface geometry, especially in a three-dimensional application.

The thermal tomography problems, including the shape or cavity estimation, have been solved by a variety of numerical methods [4–8]. Huang and his coworkers have used the gradient based algorithm together with the boundary element technique or commercial code CFD-ACE+ [9] to the inverse geometry problems and have published a series of relevant works for the two-dimensional [10–13] and three-dimensional applications [14,15]. It should be noted that the above references are all to determine the unknown boundary configurations in a single region domain. In [13], it is a multiple domain problem, but is still in determining the boundary configurations.

The thermal tomography problem in estimating the unknown interfacial configurations in a multiple region domain is very limited in the literature. This kind of approach can be applied to many engineering applications such as the interface geometry identification for the composite material and for the phase change (Stefan) problems, ice thickness estimation in a thermal storage system and crystal growth estimation, etc. Moreover, this technique can also be used to enhance the cooling rate for the composite material [16].

Recently, Huang and Shih [17] applied the techniques of the conjugate gradient method (CGM) and boundary element method to estimate the interfacial geometry in a multiple region domain. The accuracy of the thermal tomography problem is examined by using the simulated temperature measurements. Finally it is concluded that the CGM can estimate the reliable interfacial configuration.

The objective of the present inverse geometry problem is to estimate the unknown interfacial configurations in a three-dimensional multiple region domain by using the commercial code CFD-ACE+. This software is available for solving fluid dynamic and

heat transfer problems and the advantage of calling CFD-ACE+ as a subroutine in the present thermal tomography calculation lies in that its auto mesh function enables the handling of this moving boundary problem. If one can devise a thermal tomography algorithm, which has the ability to communicate with CFD-ACE+ code by means of data transportation, a generalized three-dimensional inverse geometry problem can thus be established.

The CGM is also called an iterative regularization method [18], which means the regularization procedure is performed during the iterative processes and thus the determination of optimal regularization conditions is not needed. The CGM derives from the perturbation principles and transforms the inverse geometry problem to the solution of three problems, namely, the direct, sensitivity and the adjoint problem.

These three problems can be solved by CFD-ACE+ and the calculated results are used in the CGM for thermal tomography calculations. A sequence of forward steady-state heat conduction problems is solved by CFD-ACE+ in an effort to update the interfacial geometry by minimizing a residual measuring the difference between estimated and measured temperatures at the temperature extracting locations.

Finally the solutions for this study with three different irregular interfacial geometries will be illustrated to show the validity of using the CGM in the present three-dimensional thermal tomography problem.

## II. Direct Problem

The following three-dimensional heat conduction model in a multiple region domain is considered to illustrate the methodology for developing expressions for use to determine the interfacial geometry. The boundary conditions for region $\Omega_1$ are assumed insulated at $x = 0$, $L_1$ and $y = 0$, $L_2$ and is subjected to a Robin condition at $z = 0$ with an ambient temperature,$T_{\infty h}$, and a heat transfer coefficient, $h$. Similarly, the boundary conditions for region $\Omega_2$ are also insulated at $x = 0, L_1$ and $y = 0, L_2$ and is also subjected to a Robin condition at $z = L_3$ with an ambient temperature, $T_{\infty c}$, and a heat transfer coefficient, $h$.

A perfect contact condition is applied to the interface condition on $\Gamma$, i.e., the temperature and heat flux on $\Gamma$ are the same in both $\Omega_1$ and $\Omega_2$ domains. Figure 1a shows the geometry and the coordinates and Fig. 1b indicates the grid system for the three-dimensional multiple region domains considered here.

The dimensional mathematical formulation of this three-dimensional heat conduction problem is given in region $\Omega_1$ as

$$\frac{\partial^2 T_1(\Omega_1)}{\partial x^2} + \frac{\partial^2 T_1(\Omega_1)}{\partial y^2} + \frac{\partial^2 T_1(\Omega_1)}{\partial z^2} = 0; \quad \text{in } \Omega_1 \tag{1a}$$

$$\frac{\partial T_1(\Omega_1)}{\partial x} = 0; \quad \text{at } x = 0 \quad \text{and} \quad L_1 \tag{1b}$$

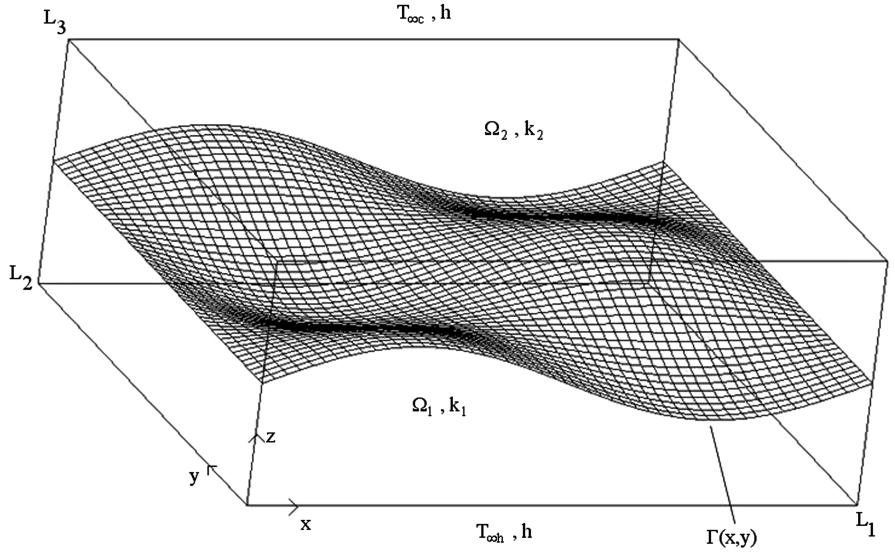


a)

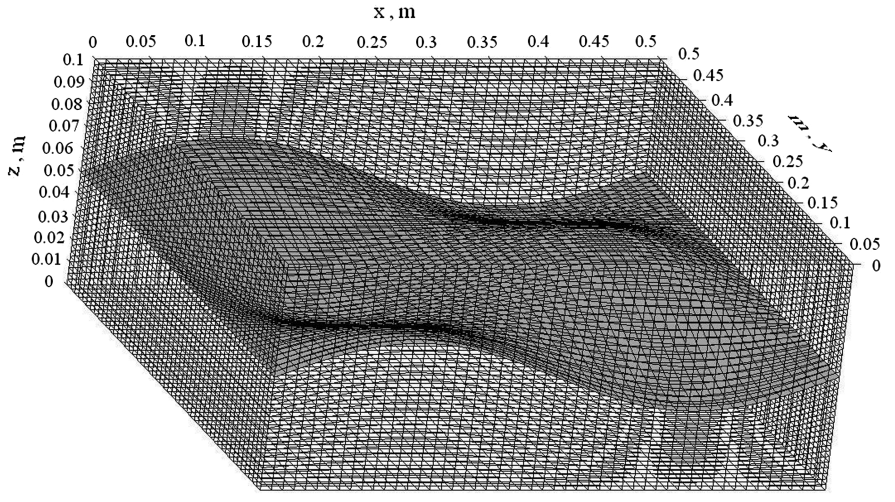


b)

**Fig. 1 The domain structure for the present study: a) geometry and coordinates and b) grid system.**

$$\frac{\partial T_1(\Omega_1)}{\partial y} = 0; \quad \text{at } y = 0 \quad \text{and} \quad L_2 \tag{1c}$$

$$-k_1 \frac{\partial T_1(\Omega_1)}{\partial z} = h(T_{\infty h} - T_1); \quad \text{at } z = 0 \tag{1d}$$

and in region $\Omega_2$ as

$$\frac{\partial^2 T_2(\Omega_2)}{\partial x^2} + \frac{\partial^2 T_2(\Omega_2)}{\partial y^2} + \frac{\partial^2 T_2(\Omega_2)}{\partial z^2} = 0; \quad \text{in } \Omega_2 \tag{2a}$$

$$\frac{\partial T_2(\Omega_2)}{\partial x} = 0; \quad \text{at } x = 0 \quad \text{and} \quad L_1 \tag{2b}$$

$$\frac{\partial T_2(\Omega_2)}{\partial y} = 0; \quad \text{at } y = 0 \quad \text{and} \quad L_2 \tag{2c}$$

$$-k_2 \frac{\partial T_2(\Omega_2)}{\partial z} = h(T_2 - T_{\infty c}); \quad \text{at } z = L_3 \tag{2d}$$

Interfacial conditions for regions $\Omega_1$ and $\Omega_2$ on $\Gamma(x, y)$ are

$$T_1(\Omega_1) = T_2(\Omega_2); \quad \text{on the unknown interface } \Gamma(x, y) \tag{3a}$$

$$k_1 \frac{\partial T_1(\Omega_1)}{\partial n} = k_2 \frac{\partial T_2(\Omega_2)}{\partial n}; \quad \text{on the unknown interface } \Gamma(x, y) \tag{3b}$$

Here subscripts 1 and 2 denote two different domains with thermal conductivity $k_1$ and $k_2$, respectively, and $n$ denotes the outward normal unit vector. The above direct problem is solved by the commercial package CFD-ACE+ for the reason that it has the function of auto mesh.

The direct problem considered here is concerned with the determination of the domain temperature distributions when the interfacial geometry on $\Gamma(x, y)$, thermal properties and the boundary conditions are given and known.

## III. Thermal Tomography Problem

For the thermal tomography problem, the interfacial geometry on $\Gamma(x, y)$ is regarded as being unknown, but everything else in direct problem, i.e. Eqs. (1–3) are known. In addition, simulated temperature readings taken by an imaginary infrared scanner on either the bottom surface $S_{\text{bottom}}$ at $z = 0$ or on the top surface $S_{\text{top}}$ at $z = L_3$ are considered available. In this work no real measured temperatures were used, instead, the simulated values of measured temperatures on $S_{\text{bottom}}$ or $S_{\text{top}}$ are generated by using the exact geometry of the interfacial surface in the solution of direct problem. Then try to retrieve the geometry of the interfacial surface by using the simulated measured temperatures on $S_{\text{bottom}}$ or $S_{\text{top}}$ and the technique of the CGM.

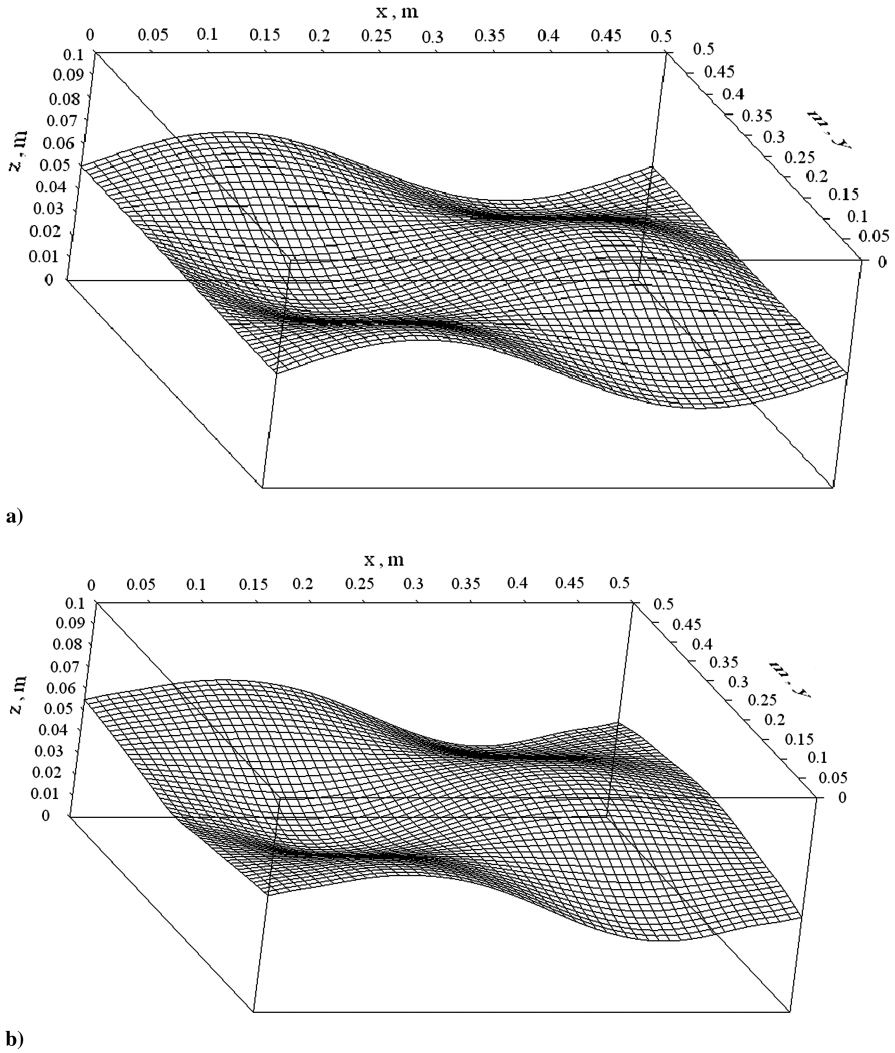


**Fig. 2 When using $\sigma = 0.0$, $\Gamma(x, y)^0 = 0.015$ m and $Y(S_{\text{bottom}})$ in case 1: a) exact and b) estimated interfacial configurations $\Gamma(x, y)$.**

Referring to Fig. 1, let the temperature reading taken by infrared scanners on the bottom surface $S_{\text{bottom}}$ be denoted by $\mathbf{Y}(S_{\text{bottom}}) \equiv Y(x_m, y_m)$, $m = 1$ to $M$, where $M$ represents the total number of extracting points for the measured temperatures. It should be noted that the measured temperature $\mathbf{Y}(S_{\text{bottom}})$ should contain measurement errors. This three-dimensional thermal tomography problem can be stated as follows: by using the above mentioned measured temperature data $\mathbf{Y}(S_{\text{bottom}})$, estimate the unknown geometry of the interfacial surface, $z = \Gamma(x, y)$.

The solution of the present thermal tomography problem is to be obtained in such a way that the following functional is minimized:

$$J[\Gamma(x,y)] = \sum_{m=1}^{M} [T_1(x_m, y_m, 0) - Y_1(x_m, y_m, 0)]^2$$
$$= \int_{y=0}^{L_2} \int_{x=0}^{L_1} [T_1(x,y,0) - Y_1(x,y,0)]^2 \delta(x - x_m)\delta(y - y_m)\,\mathrm{d}x\,\mathrm{d}y \quad (4a)$$

where $\delta(\bullet)$ is the Dirac delta function and $T_1(x_m, y_m, 0)$ are the estimated or computed temperatures at $z = 0$ at the temperature extracting points $(x_m, y_m, 0)$. These quantities are determined from the solution of the direct problem given previously by using an estimated $\Gamma(x, y)$ for the exact $\Gamma(x, y)$.

When the imaginary infrared scanners are placed at $z = L_3$, i.e., top surface, the following functional should be used:

$$J[\Gamma(x,y)] = \sum_{m=1}^{M} [T_2(x_m, y_m, L_3) - Y_2(x_m, y_m, L_3)]^2$$
$$= \int_{y=0}^{L_2} \int_{x=0}^{L_1} [T_2(x,y,L_3) - Y_2(x,y,L_3)]^2 \delta(x - x_m)\delta(y - y_m)\,\mathrm{d}x\,\mathrm{d}y \quad (4b)$$

## IV. Conjugate Gradient Method for Minimization

The following iterative regularization algorithm based on the CGM [18] is used for the estimation of unknown interfacial geometry $\Gamma(x, y)$, the expressions can be obtained as

$$\Gamma^{n+1}(x, y) = \Gamma^n(x, y) - \beta^n P^n(x, y); \quad \text{for } n = 0, 1, 2, \cdots\cdots \quad (5)$$

where $\beta^n$ is the search step size in going from iteration $n$ to iteration $n + 1$, $P^n(x, y)$ is the direction of descent (i.e. search direction) given by

$$P^n(x, y) = J'^n(x, y) + \gamma^n P^{n-1}(x, y) \quad (6)$$

which is a conjugation of the gradient direction $J'^n(x, y)$ at iteration $n$ and the direction of descent $P^{n-1}(x, y)$ at iteration $n - 1$. The conjugate coefficient is defined as

$$\gamma^n = \frac{\int_\Gamma (J'^n)^2\,\mathrm{d}\Gamma}{\int_\Gamma (J'^{n-1})^2\,\mathrm{d}\Gamma}; \quad \text{with} \quad \gamma^0 = 0 \quad (7)$$

It is noted that when $\gamma^n = 0$ for any $n$ in Eq. (6), the direction of descent $P^n(x, y)$ becomes the gradient direction, i.e., the steepest descent method is obtained. The convergence of the above iterative procedure in minimizing the functional $J$ is guaranteed in [19].

To perform the iterations according to Eq. (5), the step size $\beta^n$ and the gradient of the functional $J'^n(x, y)$ need be computed. To develop expressions for the determination of these two quantities, a "sensitivity problem" and an "adjoint problem" are constructed as described below.

### A. Sensitivity Problem and Search Step Size

The sensitivity problem is obtained from the original direct problem defined in Eqs. (1–3) by assuming that when $z = \Gamma(x, y)$ undergoes a variation $\Delta\Gamma(x, y)$ in $z$ direction only, $T_1$ and $T_2$ is perturbed by $\Delta T_1$ and $\Delta T_2$, respectively. Then replacing $\Gamma$ in the direct problem by $\Gamma + \Delta\Gamma$, $T_1$ by $T_1 + \Delta T_1$ and $T_2$ by $T_2 + \Delta T_2$, subtracting the resulting expressions from the direct problem and neglecting the second-order terms, the following sensitivity problem for the sensitivity functions $\Delta T_1$ and $\Delta T_2$ are obtained. In region $\Omega_1$,

$$\frac{\partial^2 \Delta T_1(\Omega_1)}{\partial x^2} + \frac{\partial^2 \Delta T_1(\Omega_1)}{\partial y^2} + \frac{\partial^2 \Delta T_1(\Omega_1)}{\partial z^2} = 0; \quad \text{in } \Omega_1 \quad (8a)$$

$$\frac{\partial \Delta T_1(\Omega_1)}{\partial x} = 0; \quad \text{at } x = 0 \quad \text{and} \quad L_1 \quad (8b)$$

$$\frac{\partial \Delta T_1(\Omega_1)}{\partial y} = 0; \quad \text{at } y = 0 \quad \text{and} \quad L_2 \quad (8c)$$

$$-k_1 \frac{\partial \Delta T_1(\Omega_1)}{\partial z} = -h \Delta T_1; \quad \text{at } z = 0 \quad (8d)$$

and in region $\Omega_2$,

$$\frac{\partial^2 \Delta T_2(\Omega_2)}{\partial x^2} + \frac{\partial^2 \Delta T_2(\Omega_2)}{\partial y^2} + \frac{\partial^2 \Delta T_2(\Omega_2)}{\partial z^2} = 0; \quad \text{in } \Omega_2 \quad (9a)$$

$$\frac{\partial \Delta T_2(\Omega_2)}{\partial x} = 0; \quad \text{at } x = 0 \quad \text{and} \quad L_1 \quad (9b)$$

$$\frac{\partial \Delta T_2(\Omega_2)}{\partial y} = 0; \quad \text{at } y = 0 \quad \text{and} \quad L_2 \quad (9c)$$

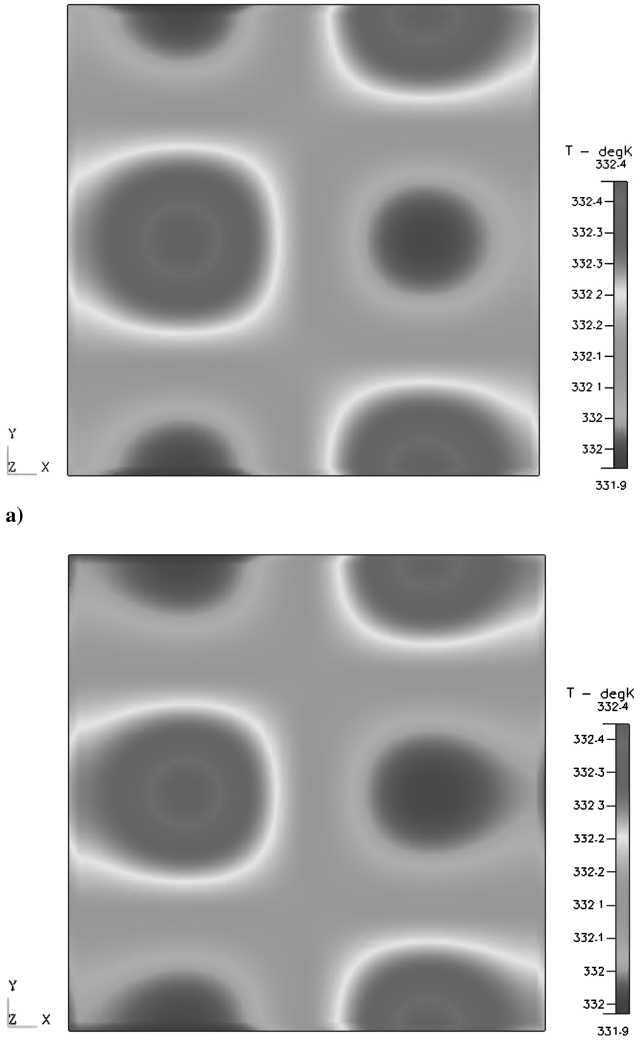


**Fig. 3 When using $\sigma = 0.0$ and $\Gamma(x, y)^0 = 0.015$ m in case 1: a) simulated measured and b) estimated surface temperatures on $S_{\text{bottom}}$.**

$$-k_2\frac{\partial \Delta T_2(\Omega_2)}{\partial z} = h\Delta T_2; \quad \text{at } z = L_3 \tag{9d}$$

Interfacial conditions for regions $\Omega_1$ and $\Omega_2$ can be obtained as

$$\Delta T_1(\Omega_1) = T_1(\Omega_1; \Gamma + \Delta\Gamma) - T_1(\Omega_1; \Gamma) \cong \Delta\Gamma\frac{\partial T_1}{\partial z}; \quad \text{on } \Gamma(x, y) \tag{10a}$$

$$\Delta T_2(\Omega_2) = T_2(\Omega_2; \Gamma + \Delta\Gamma) - T_2(\Omega_2; \Gamma) \cong \Delta\Gamma\frac{\partial T_2}{\partial z}; \quad \text{on } \Gamma(x, y) \tag{10b}$$

It should be noted that the sensitivity problems are now decoupled as two independent problems since the interfacial conditions become independent to each other now. This differs from our previous relevant works [10–15]. The above two sensitivity problems can be solved by the commercial package CFD-ACE+ separately.

Based on Eqs. (3) and (10), the following interfacial conditions can also be obtained:

$$\Delta T_1(\Omega_1) = \frac{k_2}{k_1}\Delta T_2(\Omega_2); \quad \text{on } \Gamma(x, y) \tag{11a}$$

$$k_1\frac{\partial \Delta T_1(\Omega_1)}{\partial n} = k_2\frac{\partial \Delta T_2(\Omega_2)}{\partial n}; \quad \text{on } \Gamma(x, y) \tag{11b}$$

The above two equations are needed in deriving the interfacial conditions for adjoint problem. The functional $J(\Gamma^{n+1})$ for iteration $n + 1$ is obtained by rewriting Eq. (4a) as

$$J(\Gamma^{n+1}) = \sum_{m=1}^{M}[T_1(x_m, y_m, 0; \Gamma^n - \beta^n P^n) - Y_1(x_m, y_m, 0)]^2 \tag{12}$$

where we have replaced $\Gamma^{n+1}$ by the expression given by Eq. (5). If temperature $T_1(x_m, y_m, 0; \Gamma^n - \beta^n P^n)$ is linearized by a Taylor expansion, Eq. (12) takes the form

$$J(\Gamma^{n+1}) = \sum_{m=1}^{M}[T_1(x_m, y_m, 0; \Gamma^n) - \beta^n \Delta T_1(x_m, y_m, 0; P^n) - Y_1(x_m, y_m, 0)]^2 \tag{13}$$

where $T_1(x_m, y_m, 0; \Gamma^n)$ is the solution of the direct problem by using the estimate $\Gamma(x, y)$ for exact $\Gamma(x, y)$ at the measured positions $(x_m, y_m, 0)$. The sensitivity function $\Delta T_1(x_m, y_m, 0; P^n)$ is taken as the solutions of problems (8–10) at the measured positions $(x_m, y_m, 0)$ by letting $\Delta\Gamma = P^n$.

The search step size $\beta^n$ is determined by minimizing the functional given by Eq. (13) with respect to $\beta^n$. Finally the following expression can be obtained:

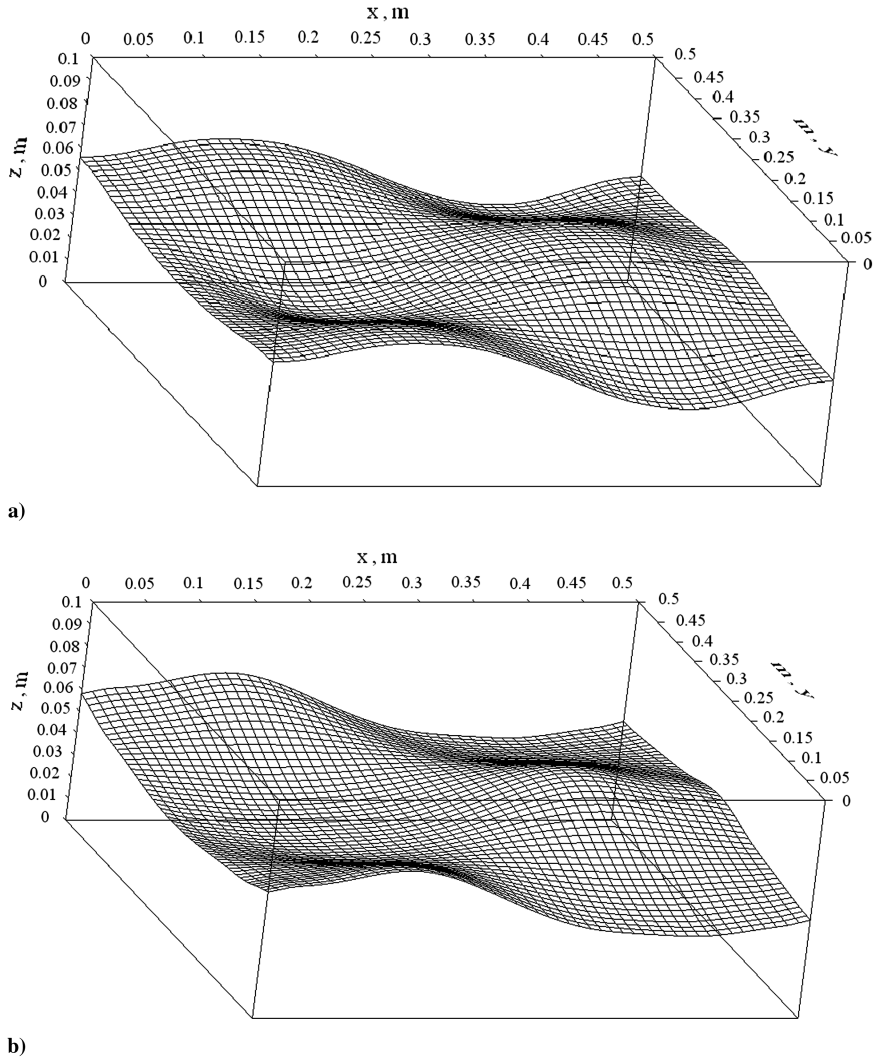


**Fig. 4 The estimated interfacial configurations $\Gamma(x, y)$ using $\sigma = 0.0$ and a) $\Gamma(x, y)^0 = 0.085$ m and $Y(S_{bottom})$ and b) $\Gamma(x, y)^0 = 0.015$ m and $Y(S_{top})$ in case 1.**

$$\beta^n = \frac{\sum_{m=1}^{M}[T_1(x_m, y_m, 0) - Y_1(x_m, y_m, 0)]\Delta T_1(x_m, y_m, 0)}{\sum_{m=1}^{M}[\Delta T_1(x_m, y_m, 0)^2]} \quad (14)$$

When the imaginary infrared scanners are placed at $z = L_3$, i.e., on top surface $S_{\text{top}}$, $T_1$, $Y_1$ and 0 should be replaced by $T_2$, $Y_2$ and $L_3$ in Eq. (14), respectively.

### B. Adjoint Problem and Gradient Equation

To obtain the adjoint problems, Eqs. (1a) and (2a) are multiplied by the Lagrange multipliers (or adjoint functions) $\lambda_1(\Omega_1)$ and $\lambda_2(\Omega_2)$, respectively, and the resulting expression is integrated over the corresponding space domains. The result is then added to the right-hand side of Eq. (4a) to yield the following expression for the functional $J[\Gamma(x, y)]$:

$$\begin{aligned} J[\Gamma(x,y)] = &\int_{y=0}^{L_2}\int_{x=0}^{L_1}[T_1(x,y,0) \\ &- Y_1(x,y,0)]^2\delta(x-x_m)\delta(y-y_m)\,\mathrm{d}x\,\mathrm{d}y \\ &+ \int_{\Omega_1}\lambda_1\left\{\frac{\partial^2 T_1}{\partial x^2} + \frac{\partial^2 T_1}{\partial y^2} + \frac{\partial^2 T_1}{\partial z^2}\right\}\mathrm{d}\Omega_1 \\ &+ \int_{\Omega_2}\lambda_2\left\{\frac{\partial^2 T_2}{\partial x^2} + \frac{\partial^2 T_2}{\partial y^2} + \frac{\partial^2 T_2}{\partial z^2}\right\}\mathrm{d}\Omega_2 \end{aligned} \quad (15)$$

The variation $\Delta J$ is obtained by perturbing $\Gamma$ by $\Delta\Gamma$, $T_1$ by $\Delta T_1$ and $T_2$ by $\Delta T_2$ in Eq. (15), subtracting the resulting expression from the original Eq. (15) and neglecting the second-order terms. This yields

$$\begin{aligned} \Delta J = &\int_{y=0}^{L_2}\int_{x=0}^{L_1} 2(T_1 - Y_1)\Delta T\delta(x-x_m)\delta(y-y_m)\,\mathrm{d}x\,\mathrm{d}y \\ &+ \int_{\Omega_1}\lambda_1\left[\frac{\partial^2\Delta T_1}{\partial x^2} + \frac{\partial^2\Delta T_1}{\partial y^2} + \frac{\partial^2\Delta T_1}{\partial z^2}\right]\mathrm{d}\Omega_1 \\ &+ \int_{\Omega_2}\lambda_2\left[\frac{\partial^2\Delta T_2}{\partial x^2} + \frac{\partial^2\Delta T_2}{\partial y^2} + \frac{\partial^2\Delta T_2}{\partial z^2}\right]\mathrm{d}\Omega_2 \end{aligned} \quad (16)$$

In Eq. (16), the domain integral term is reformulated based on Green's second identity; the boundary conditions of the sensitivity problems are used and then $\Delta J$ is allowed to go to zero. The vanishing of the integrands containing $\Delta T_1$ and $\Delta T_2$ leads to the following adjoint problems for determining the values of $\lambda_1(\Omega_1)$ and $\lambda_2(\Omega_2)$. In region $\Omega_1$,

$$\frac{\partial^2\lambda_1(\Omega_1)}{\partial x^2} + \frac{\partial^2\lambda_1(\Omega_1)}{\partial y^2} + \frac{\partial^2\lambda_1(\Omega_1)}{\partial z^2} = 0; \quad \text{in } \Omega_1 \quad (17a)$$

$$\frac{\partial\lambda_1(\Omega_1)}{\partial x} = 0; \quad \text{at } x = 0 \quad \text{and} \quad L_1 \quad (17b)$$

$$\frac{\partial\lambda_1(\Omega_1)}{\partial y} = 0; \quad \text{at } y = 0 \quad \text{and} \quad L_2 \quad (17c)$$

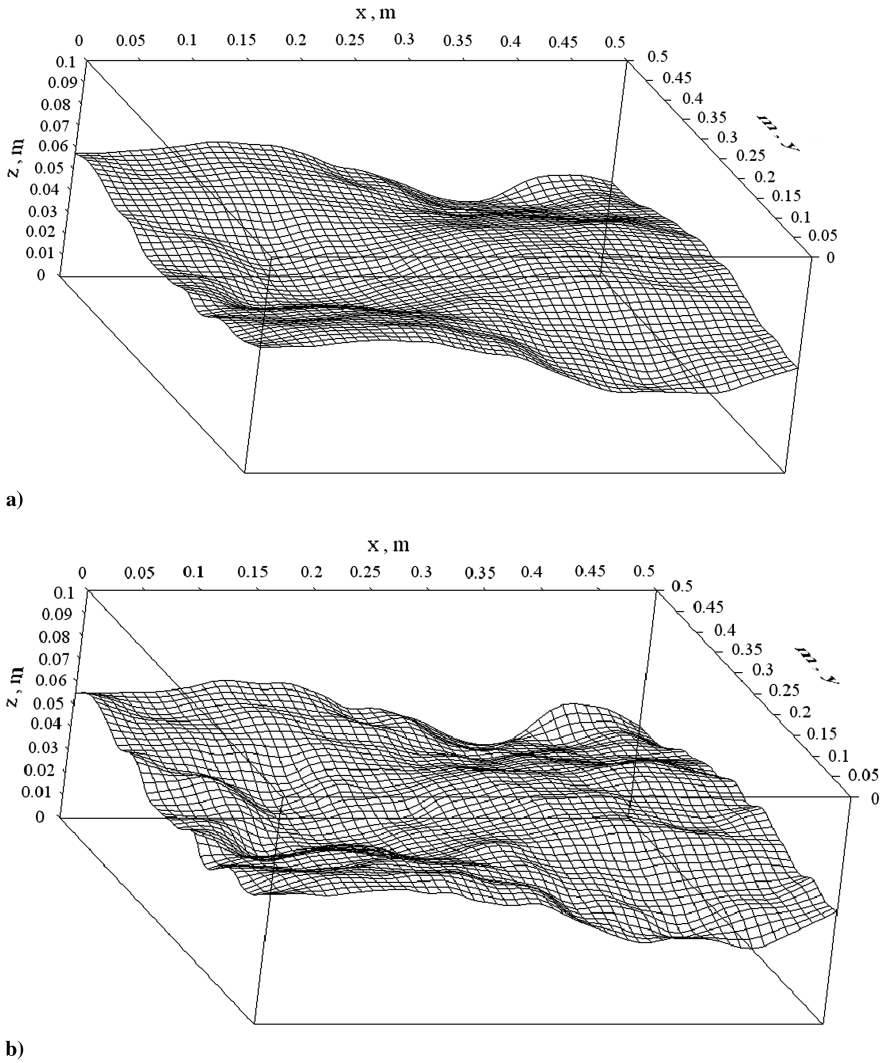


**Fig. 5 The estimated interfacial configurations $\Gamma(x, y)$ with $\Gamma(x, y)^0 = 0.015$ m and $Y(S_{\text{bottom}})$ in case 1 using a) $\sigma = 0.1$ and b) $\sigma = 0.2$.**

$$-\frac{\partial\lambda_1(\Omega_1)}{\partial z}=-\frac{h}{k_1}\lambda_1 + 2[T_1-Y_1]\delta(x-x_m)\delta(y-y_m); \quad \text{at } y=0 \tag{17d}$$

In region $\Omega_2$,

$$\frac{\partial^2\lambda_2(\Omega_2)}{\partial x^2}+\frac{\partial^2\lambda_2(\Omega_2)}{\partial y^2}+\frac{\partial^2\lambda_2(\Omega_2)}{\partial z^2}=0; \quad \text{in } \Omega_2 \tag{18a}$$

$$\frac{\partial\lambda_2(\Omega_2)}{\partial x}=0; \quad \text{at } x=0 \quad \text{and} \quad L_1 \tag{18b}$$

$$\frac{\partial\lambda_2(\Omega_2)}{\partial y}=0; \quad \text{at } y=0 \quad \text{and} \quad L_2 \tag{18c}$$

$$-\frac{\partial\lambda_2(\Omega_2)}{\partial z}=\frac{h}{k_2}\lambda_2; \quad \text{at } z=L_3 \tag{18d}$$

Interfacial conditions for regions $\Omega_1$ and $\Omega_2$ are

$$\lambda_1(\Omega_1)=\frac{k_1}{k_2}\lambda_2(\Omega_2); \quad \text{on } \Gamma(x,y) \tag{19a}$$

$$k_2\frac{\partial\lambda_1(\Omega_1)}{\partial n}=k_1\frac{\partial\lambda_2(\Omega_2)}{\partial n}; \quad \text{on } \Gamma(x,y) \tag{19b}$$

It should be noted that when the imaginary infrared scanners are placed at $z=L_3$, i.e., upper surface, the term $2[T_1-Y_1]\delta(x-x_m)\delta(y-y_m)$ should be moved from Eq. (17d) and the term $2[T_2-Y_2]\delta(x-x_m)\delta(y-y_m)$ should be added to the right-hand side of Eq. (18d). The commercial package CFD-ACE+ is used to solve the above adjoint problems.

Finally all terms are used to set up the above complete expressions for adjoint problems and nothing is left for the determination of gradient equation. This also differs from our previous relevant studies [10–15]. One of the used integral terms obtained from the integration by parts should be used again in determining the gradient equation; this term is defined as an overused condition.

The integral term containing $\Delta\Gamma(x,y)$ should be used again to obtain the expression of gradient equation for use in the conjugate gradient algorithm, even thought it was used implicitly as the interfacial condition to obtain Eq. (19b). Finally the following expression can be obtained:

$$\Delta J=\int_\Gamma\left[-\frac{\partial T_1}{\partial z}\frac{\partial\lambda_1}{\partial n}\right]_\Gamma\Delta\Gamma\,d\Gamma \tag{20a}$$

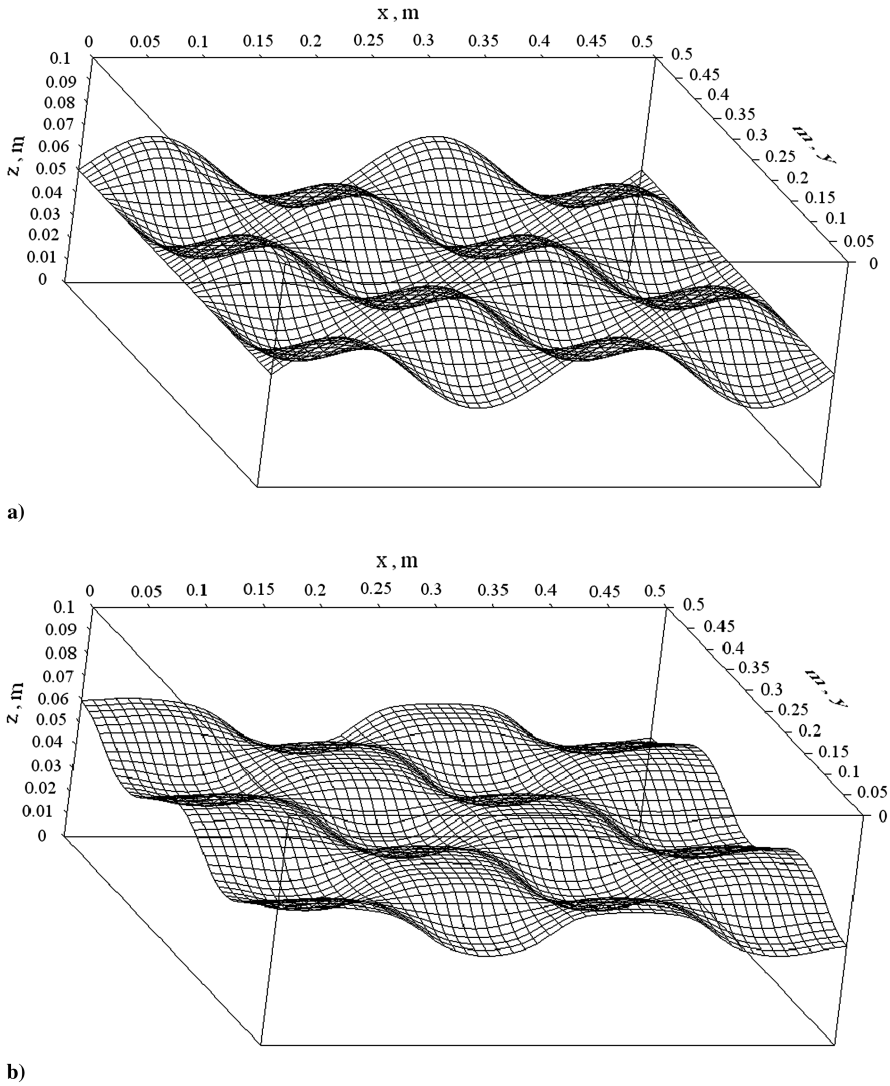


**Fig. 6 When using $\sigma=0.0$, $\Gamma(x,y)^0=0.015$ m and $Y(S_{\text{bottom}})$ in case 2: a) exact and b) estimated interfacial configurations $\Gamma(x,y)$.**

From definition [18], the functional increment can be presented as

$$\Delta J = \int_{\Gamma} J'(x,y)\Delta\Gamma \, d\Gamma \tag{20b}$$

A comparison of Eqs. (20a) and (20b) leads to the following expression for the gradient of functional $J'(x)$ of the functional $J[\Gamma(x,y)]$:

$$J'(x,y) = -\frac{\partial T_1}{\partial z}\frac{\partial \lambda_1}{\partial n}\bigg|_{\Gamma} \tag{21a}$$

Similarly, when the imaginary infrared scanners are placed at $z = L_3$, the following gradient equation should be applied:

$$J'(x,y) = -\frac{\partial T_2}{\partial z}\frac{\partial \lambda_2}{\partial n}\bigg|_{\Gamma} \tag{21b}$$

### C. Stopping Criterion

If the problem contains no measurement errors, the traditional check condition is specified as

$$J[\Gamma^{n+1}(x,y)] < \varepsilon \tag{22a}$$

where $\varepsilon$ is a small-specified number. However, the observed temperature data may contain measurement errors. For this reason we do not expect the functional Eq. (4) to be equal to zero at the final iteration step. Following the experiences of the authors in [10–15,18], the discrepancy principle can be applied as the stopping criterion, i.e., it is assumed that the temperature residuals may be approximated by

$$T_1(x_m, y_m, 0) - Y_1(x_m, y_m, 0) \approx \sigma \tag{22b}$$

where $\sigma$ is the standard deviation of the measurements, which is assumed to be a constant. Substituting Eq. (22b) into Eq. (4), the following expression is obtained for stopping criteria $\varepsilon$:

$$\varepsilon = M\sigma^2 \tag{22c}$$

## V. Computational Procedure

The computational procedure for the solution of this thermal tomography problem using CGM may be summarized as follows:

Suppose $\Gamma^n(x,y)$ is available at iteration $n$:

1) Solve the direct problem given by Eqs. (1–3) for $T_1(\Omega_1)$ and $T_2(\Omega_2)$.

2) Check the stopping criterion given by Eq. (22a) with $\varepsilon$ given by Eq. (22c). Continue if not satisfied.

3) Solve the adjoint problems given by Eqs. (17–19) for $\lambda_1(\Omega_1)$ and $\lambda_2(\Omega_2)$.

4) Compute the gradient of the functional $J'$ from Eq. (21).

5) Compute the conjugate coefficient $\gamma^n$ and direction of descent $P^n$ from Eqs. (7) and (6), respectively.

6) Set $\Delta\Gamma(x,y) = P^n(x,y)$, and solve the sensitivity problems given by Eqs. (8–10) for $\Delta T_1(\Omega_1)$ and $\Delta T_2(\Omega_2)$.

7) Compute the search step size $\beta^n$ from Eq. (14).

8) Compute the new estimation for $\Gamma^{n+1}(x,y)$ from Eq. (5) and return to step 1.

## VI. Results and Discussions

To examine the validity of the present thermal tomography algorithms in determining interfacial surface configuration $\Gamma(x,y)$ for a multiple region domain from the knowledge of temperature recordings by an imaginary infrared scanner, three specific examples are considered where the boundary geometry on $\Gamma(x,y)$ is assumed as a mixed trigonometry function or a step function, respectively. The goal of the present work is to show the accuracy of this algorithm in estimating interfacial configuration $\Gamma(x,y)$ with no prior information on the functional form of the unknown quantities.

To compare the results for situations when measurement errors are considered randomly, the normally distributed uncorrelated errors with zero mean and constant standard deviation are considered in this work. The simulated inexact measurement data $\mathbf{Y}$ can thus be expressed as

$$\mathbf{Y} = \mathbf{Y}_{\text{exact}} + \omega\sigma \tag{23}$$

where $\mathbf{Y}_{\text{exact}}$ is the solution of direct problem on the measurement surface with an exact $\Gamma(x,y)$; $\sigma$ is the standard deviation of the measurements; and $\omega$ is a random variable that generated by subroutine DRNNOR of the IMSL [20] and will be within $-2.576$ to 2.576 for the 99% confidence bounds.

When the depth of the interface from the measuring surface is large, the temperature distribution on the measuring surface becomes irrelevant to the shape of interface and this makes it impossible to identify the shape of interfacial surface. In all the test cases considered here we have chosen $L_1$(length in $x$ direction)$=$ $L_2$(length in $y$ direction) $= 0.5$ m, $L_3$(length in $z$ direction)$=$ 0.1 m, $T_{\infty h} = 100°$C, $T_{\infty c} = 10°$C, $k_1 = 190$ W/m-K, $k_2 = 48$ W/m-K and $h = 150$ W/m$^2$-K. The grid number in $x$, $y$ and $z$ directions are taken as $51 \times 51 \times 41$. The imaginary infrared scanner be placed either on $z = 0$, i.e., on the bottom surface, or on $z = L_3$, i.e., on the top surface.

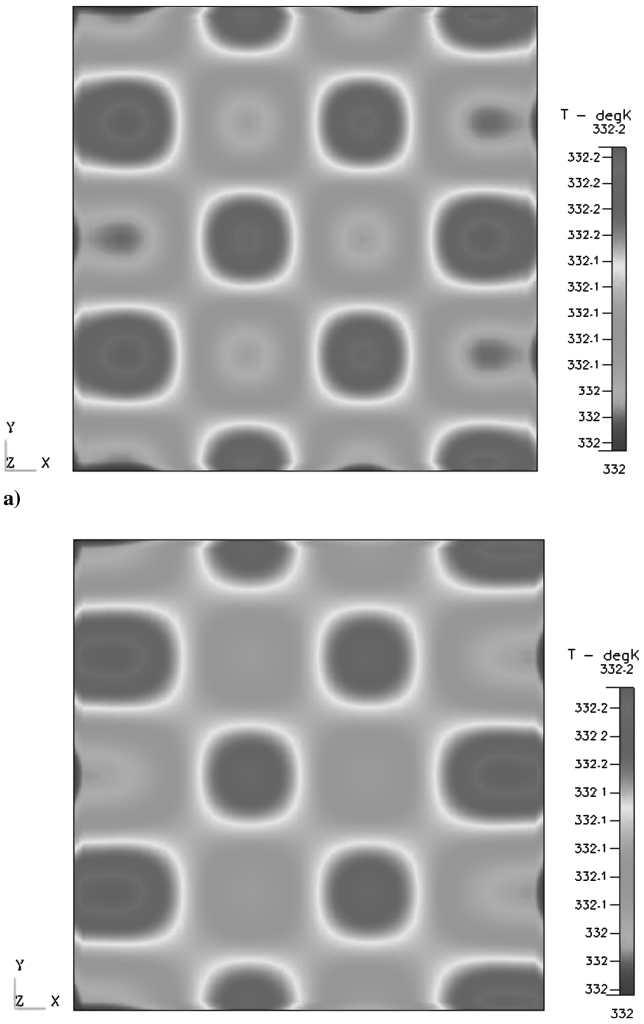


**Fig. 7 When using $\sigma = 0.0$ and $\Gamma(x,y)^0 = 0.015$ m in case 2: a) simulated measured and b) estimated surface temperatures on $S_{\text{bottom}}$.**

Three numerical experiments in determining $\Gamma(x, y)$ by the present inverse analysis are presented below:

### A. Numerical Test Case 1

The unknown interfacial configuration at $z = \Gamma(x, y)$ is assumed to vary with $x$ and $y$ in the following form:

$$\Gamma(x, y) = 0.05 + 0.015 \times \sin(4\pi x) \times \cos(4\pi x); \quad 0 \le x, y \le 0.5 \text{ m} \tag{24}$$

Firstly the inverse analysis is performed by assuming exact measurements, i. e. $\sigma = 0.0$, $\Gamma(x, y)^0 = 0.015$ m and the imaginary infrared scanner is placed on $z = 0$, i.e., on the bottom surface. By setting convergent criterion $\varepsilon = 0.5$ and after eight iterations the shape of interfacial surface $\Gamma(x, y)$ can be estimated.

The exact and estimated shapes of $\Gamma(x, y)$ by using CGM are shown in Figs. 2a and 2b, respectively, while the measured and estimated surface temperatures on $S_{\text{bottom}}$ are illustrated in Figs. 3a and 3b, respectively.

The average relative errors for the exact and estimated surface configurations and for the measured and estimated temperatures are calculated ERR1 $= 1.711\%$ and ERR2 $= 0.003\%$, respectively, where the average relative errors ERR1 and ERR2 are defined as

$$\text{ERR 1} = \sum_{n=1}^{N}\sum_{m=1}^{M}\left|\frac{\Gamma(x_n, y_m) - \hat{\Gamma}(x_n, y_m)}{\Gamma(x_n, y_m)}\right| \div (N \times M) \times 100\% \tag{25a}$$

$$\text{ERR 2} = \sum_{n=1}^{N}\sum_{m=1}^{M}\left|\frac{T(x_n, y_m) - Y(x_n, y_m)}{Y(x_n, y_m)}\right| \div (N \times M) \times 100\% \tag{25b}$$

Here $N = 51$ and $M = 51$ represent the total discreted number of grid in $x$ and $y$ directions, respectively, and $(N \times M)$ indicates the total number of the unknown parameters, while $\Gamma$ and $\hat{\Gamma}$ denote the exact and estimated values of interfacial surface configurations.

It is clear from the above figures and relative average errors that the present inverse scheme obtained good estimation for $\Gamma(x, y)$ and the CPU time on Pentium IV-3 GHz PC is about 320 min.

Next it is of interest to examine the estimation by using different initial guess as well as different measured position. When considering $\Gamma(x, y)^0 = 0.085$ m, after nine iterations the shape of interfacial surface $\Gamma(x, y)$ can be estimated and it is plotted in Fig. 4a. The average relative errors are calculated ERR1 $= 1.758\%$ and ERR2 $= 0.003\%$, respectively. Then the measured position is switched to $z = L_3$, i.e., on the top surface and performed the same inverse calculations also using $\Gamma(x, y)^0 = 0.085$ m. After 11 iterations the interfacial surface $\Gamma(x, y)$ can be estimated and is shown in Fig. 4b. The average relative errors are calculated ERR1 $= 2.810\%$ and ERR2 $= 0.012\%$, respectively.

Based on the estimated results of the above numerical experiments it was found that when the condition of no measurement error, i.e. $\sigma = 0.0$, is considered, a very accurate interfacial geometry can be obtained by varying initial guess as well as measured position.

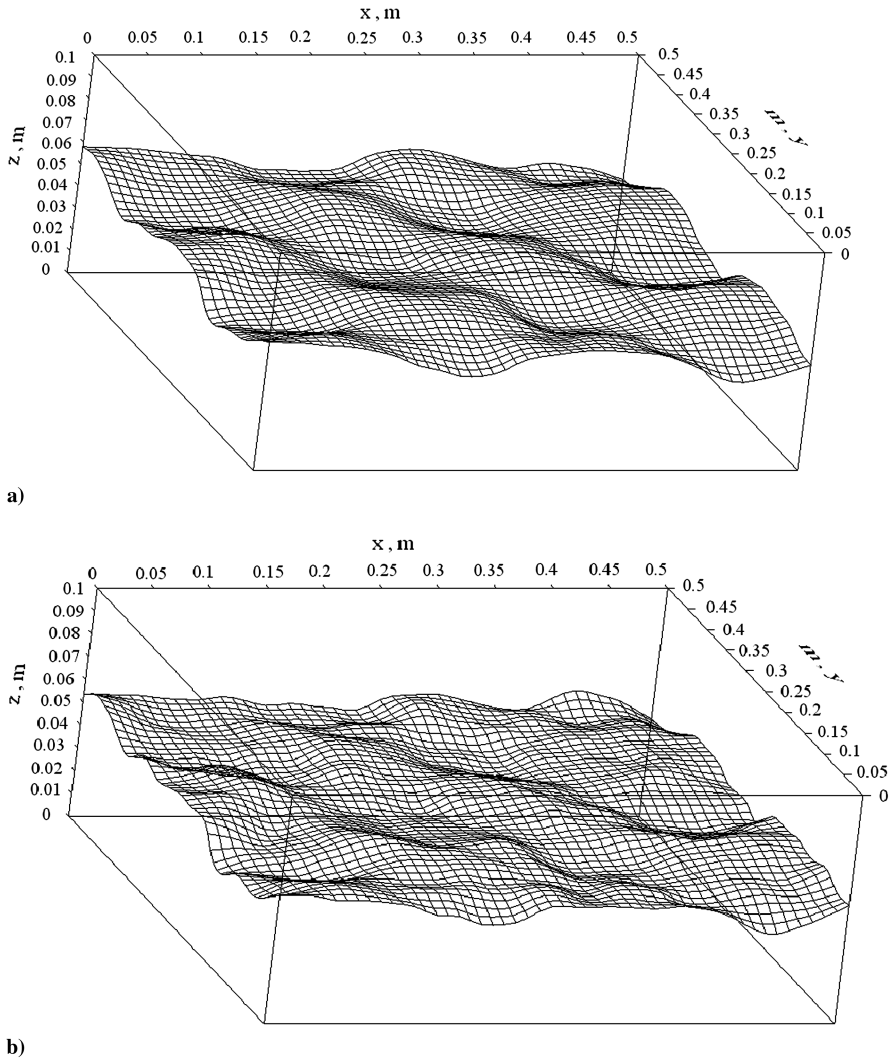


**Fig. 8 The estimated interfacial configurations $\Gamma(x, y)$ with $\Gamma(x, y)^0 = 0.015$ m and $Y(S_{\text{bottom}})$ in case 2 using a) $\sigma = 0.1$ and b) $\sigma = 0.2$.**

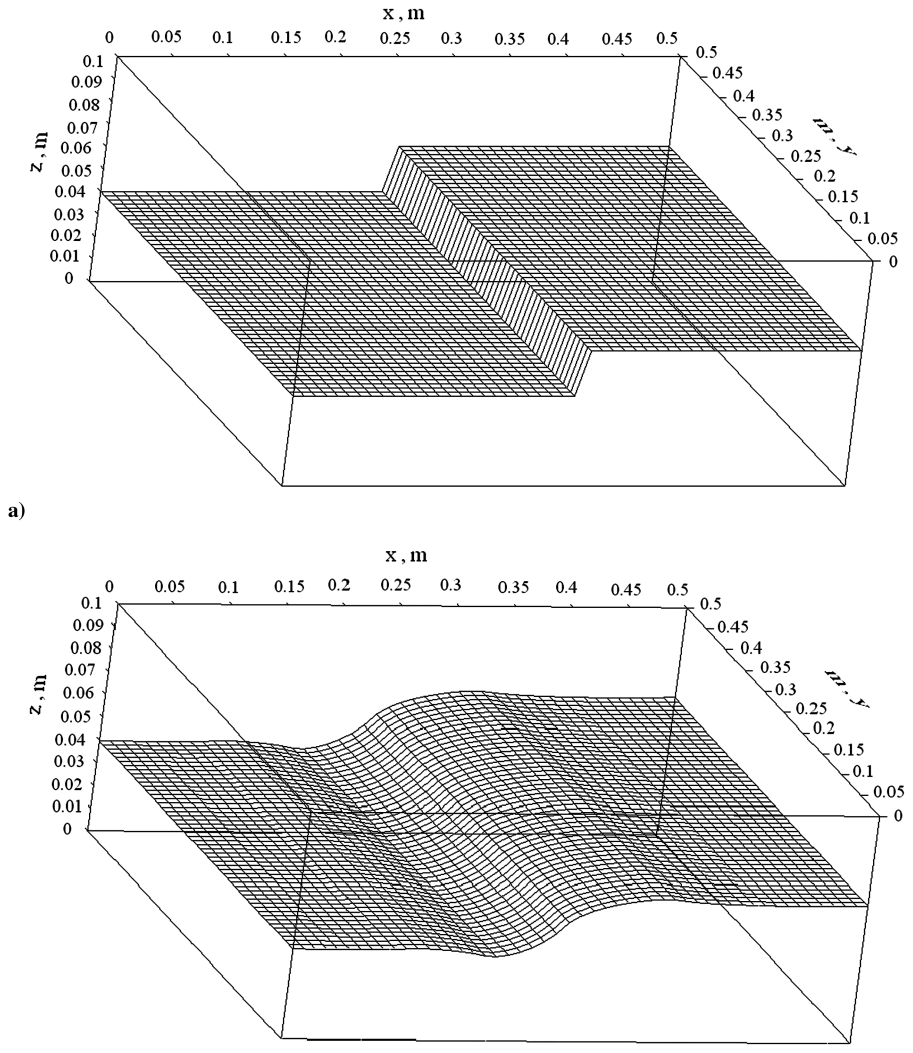


**Fig. 9 When using $\sigma = 0.0$, $\Gamma(x,y)^0 = 0.015$ m and $Y(S_{bottom})$ in case 3: a) exact and b) estimated interfacial configurations $\Gamma(x,y)$.**

Finally, let us discuss the influence of the measurement errors on the inverse solutions. First, the measurement error for the simulated temperatures measured by infrared scanners on bottom surface $S_{bottom}$ is taken as $\sigma = 0.1$. The estimation for $\Gamma(x, y)$ can be obtained after only six iterations (CPU time is about 240 min) and is plotted in Fig. 5a. The relative average errors ERR1 and ERR2 are calculated as ERR1 = 3.646% and ERR2 = 0.024%, respectively. The measurement error for the temperatures is then increased to $\sigma = 0.2$. After only five iterations (CPU time is about 200 min) the estimated $\Gamma(x, y)$ is obtained and illustrated in Fig. 5b. ERR1 and ERR2 are calculated as 4.710 and 0.046%, respectively. From the above results it can be concluded that the reliable inverse solutions can still be obtained when reasonable measurement errors are considered.

### B. Numerical Test Case 2

In the second test case, $\Gamma(x, y)$ is taken as

$$\Gamma(x, y) = 0.05 + 0.015 \times \sin(8\pi x) \times \cos(8\pi x); \quad 0 \le x, y \le 0.5 \text{ m} \tag{26}$$

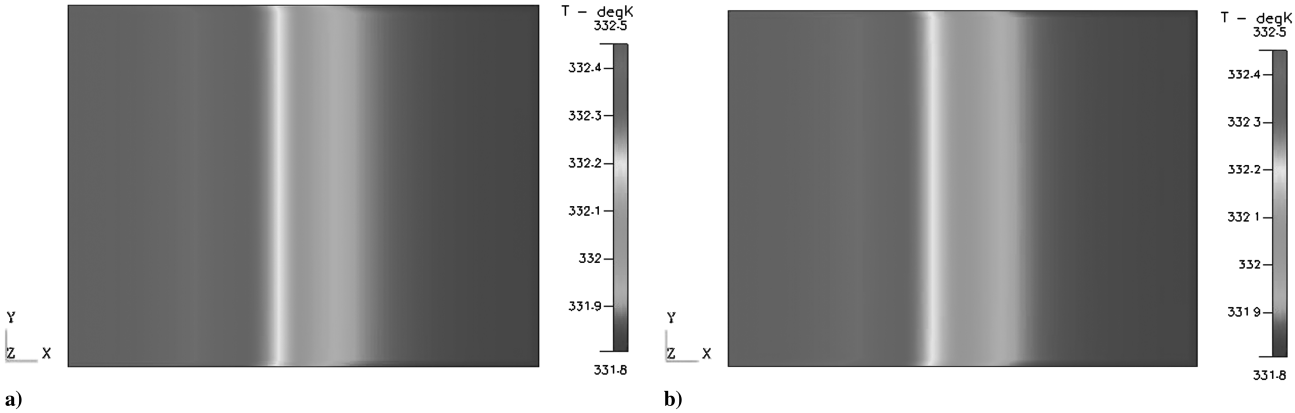


**Fig. 10 When using $\sigma = 0.0$ and $\Gamma(x,y)^0 = 0.015$ m in case 3: a) simulated measured and b) estimated surface temperatures on $S_{bottom}$.**

This shape of interfacial surface represents more oscillatory behavior than in case 1. The imaginary infrared scanner is also placed on the bottom surface and $\Gamma(x, y)^0 = 0.015$ m is used in the calculations.

The inverse analysis is first performed by assuming $\sigma = 0.0$, by setting convergent criterion $\varepsilon = 0.5$ and after 25 iterations the shape of interfacial surface $\Gamma(x, y)$ can be estimated. The exact and estimated shapes of $\Gamma(x, y)$ are shown in Figs. 6a and 6b, respectively, and the measured and estimated surface temperatures on $S_{\text{bottom}}$ are illustrated in Figs. 7a and 7b, respectively. The average relative errors for the exact and estimated surface configurations and for the measured and estimated temperatures are calculated ERR1 = 4.141% and ERR2 = 0.003%, respectively.

Next, error measurement will be considered in the numerical experiments. First, the measurement error for the simulated temperatures measured by infrared scanners on the bottom surface $S_{\text{bottom}}$ is taken as $\sigma = 0.1$. After eight iterations (CPU time is about 320 min), the estimated $\Gamma(x, y)$ can be obtained and shown in Fig. 8a. The relative average errors ERR1 and ERR2 are calculated as ERR1 = 8.304% and ERR2 = 0.024%, respectively. Then, the measurement error for the temperatures is increased to $\sigma = 0.2$. The estimated $\Gamma(x, y)$ can be obtained after only five iterations (CPU time is about 200 min) and plotted in Fig. 8b. ERR1 and ERR2 are calculated as 9.732% and 0.047%, respectively. From Figs. 8a and 8b we concluded that the reliable inverse solutions can still be obtained when large measurement errors are included. Again, this implies that the CGM is not sensitive to the measurement errors.

### C. Numerical Test Case 3

In the third test case, a stricter $\Gamma(x, y)$ is taken as a step function, i.e.,

$$\Gamma(x, y) = \begin{cases} 0.04; & 0 \le x, y < 0.25 \text{ m} \\ 0.06; & 0.25 \le x, y < 0.5 \text{ m} \end{cases} \tag{27}$$

The imaginary infrared scanner is placed on the bottom surface and $\Gamma(x, y)^0 = 0.015$ m is used in the calculations like numerical test case 2.

First, the inverse calculation is performed by considering $\sigma = 0.0$ and $\varepsilon = 0.5$. After 12 iterations the shape of interfacial surface $\Gamma(x, y)$ can be estimated. The exact and estimated shapes of $\Gamma(x, y)$ are shown in Figs. 9a and 9b, respectively. The measured and estimated surface temperatures on $S_{\text{bottom}}$ are illustrated in Figs. 10a and 10b, respectively. ERR1 and ERR2 are obtained as ERR1 = 3.496% and ERR2 = 0.003%, respectively.

Error measurements are then considered in the numerical experiments. The measurement error with $\sigma = 0.1$ is included. After six iterations (CPU time is about 240 min), the estimated $\Gamma(x, y)$ is obtained and shown in Fig. 11a. The relative average errors ERR1 and ERR2 are calculated as ERR1 = 4.988% and ERR2 = 0.026%, respectively. Then $\sigma = 0.2$ is considered and the estimated $\Gamma(x, y)$ can be obtained after only five iterations (CPU time is about 200 min). The result is given in Fig. 11b and ERR1 and ERR2 are

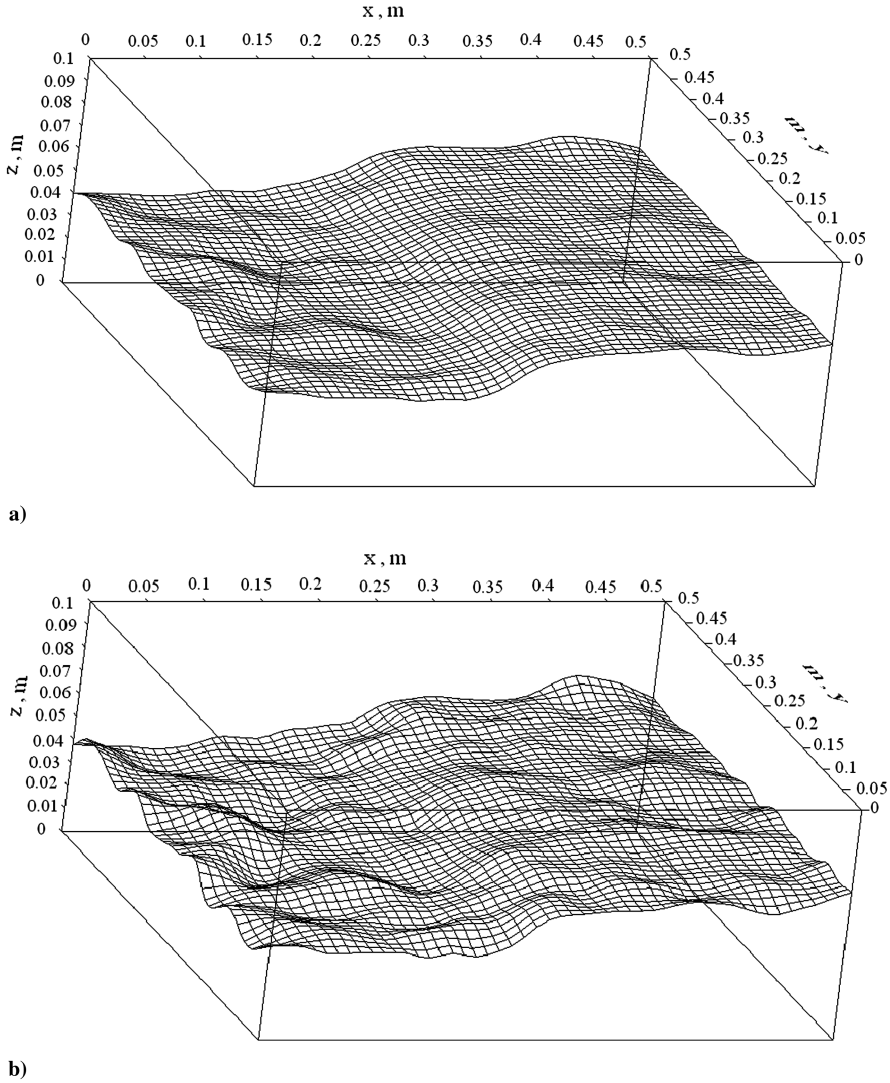


**Fig. 11 The estimated interfacial configurations $\Gamma(x, y)$ with $\Gamma(x, y)^0 = 0.015$ m and $Y(S_{\text{bottom}})$ in case 3 using a) $\sigma = 0.1$ and b) $\sigma = 0.2$.**

calculated as 6.098 and 0.046%, respectively. Again, this implies that the CGM is not sensitive to the measurement errors.

From the above three numerical test cases, it was concluded that the CGM is now applied successfully in this three-dimensional shape identification problem for predicting the unknown interfacial surface configurations.

## VII. Conclusions

The present three-dimensional thermal tomography problem in estimating the unknown interfacial surface for a multiple region domain using the Conjugate Gradient Method was successfully examined by using simulated temperature readings. Several test cases involving different functional forms of the unknown interfacial configuration, different measurement positions and errors were considered. The results show that when considering exact measurement very accurate estimation can always be obtained. When measurement errors were included, reliable estimation can still be obtained and this makes the present algorithm has the superiority in executing the thermal tomography problems.

## Acknowledgment

This work was supported in part through the National Science Council, Republic of China, Grant number NSC-97-2221-E-006-262-MY3.

## References

[1] Huang, C. H., Yan, J. Y., and Chen, H. T., "The Function Estimation in Predicting Temperature Dependent Thermal Conductivity Without Internal Measurements," *Journal of Thermophysics and Heat Transfer*, Vol. 9, No. 4, 1995, pp. 667–673. doi:10.2514/3.722

[2] Huang, C. H., and Lin, C. Y., "Inverse Hyperbolic Conduction Problem in Estimating Two Unknown Surface Heat Fluxes Simultaneously," *Journal of Thermophysics and Heat Transfer*, Vol. 22, No. 4, 2008, pp. 766–774. doi:10.2514/1.36331

[3] Huang, C. H., and Cheng, S. C., "A Three-Dimensional Inverse Problem of Estimating the Volumetric Heat Generation for a Composite Material," *Numerical Heat Transfer*, Part A, Vol. 39, No. 4, 2001, pp. 383–403. doi:10.1080/10407780151063179

[4] Burczynski, T., Beluch, W., Dlugosz, A., Kus, W., Nowakowski, M., and Orantek, P., "Evolutionary Computation in Optimization and Identification," *Computer Assisted Mechanics and Engineering Sciences*, Vol. 9, No. 1, 2002, pp. 3–20.

[5] Burczinski, T., Kane, J. H., and Balakrishna, C., "Shape Design Sensitivity Analysis via Material Derivative-Adjoint Variable Technique for 3D and 2D Curved Boundary Elements," *International Journal for Numerical Methods in Engineering*, Vol. 38, No. 17, 1995, pp. 2839–2866. doi:10.1002/nme.1620381702

[6] Park, H. M., and Shin, H. J., "Shape Identification for Natural Convection Problems Using the Adjoint Variable Method," *Journal of Computational Physics*, Vol. 186, No. 1, 2003, pp. 198–211. doi:10.1016/S0021-9991(03)00046-9

[7] Cheng, C. H., and Chang, M. H., "A Simplified Conjugate-Gradient Method for Shape Identification Based on Thermal Data," *Numerical Heat Transfer*, Part B, Vol. 43, No. 5, 2003, pp. 489–507. doi:10.1080/713836242

[8] Divo, E., Kassab, A. J., and Rodriquez, F., "An Efficient Singular Superposition Technique for Cavity Detection and Shape Optimization," *Numerical Heat Transfer*, Part B, Vol. 46, No. 1, 2004, pp. 1–30. doi:10.1080/10407790490436624

[9] CFD-ACE+ User's Manual, ESI-CFD, Inc., 2005.

[10] Huang, C. H., and Chao, B. H., "An Inverse Geometry Problem in Identifying Irregular Boundary Configurations," *International Journal of Heat and Mass Transfer*, Vol. 40, No. 9, 1997, pp. 2045–2053. doi:10.1016/S0017-9310(96)00280-3

[11] Huang, C. H., and Tsai, C. C., "A Transient Inverse Two-Dimensional Geometry Problem in Estimating Time-Dependent Irregular Boundary Configurations," *International Journal of Heat and Mass Transfer*, Vol. 41, No. 12, 1998, pp. 1707–1718. doi:10.1016/S0017-9310(97)00266-4

[12] Huang, C. H., Chiang, C. C., and Chen, H. M., "Shape Identification Problem in Estimating the Geometry of Multiple Cavities," *Journal of Thermophysics and Heat Transfer*, Vol. 12, No. 2, 1998, pp. 270–277. doi:10.2514/2.6331

[13] Huang, C. H., and Chen, H. M., "An Inverse Geometry Problem of Identifying Growth of Boundary Shapes in a Multiple Region Domain," *Numerical Heat Transfer*, Part A, Vol. 35, No. 4, 1999, pp. 435–450. doi:10.1080/104077899275218

[14] Huang, C. H., and Chaing, M. T., "A Three Dimensional Inverse Geometry Problem in Identifying Irregular Boundary Configurations," *International Journal of Thermal Sciences*, Vol. 48, No. 3, 2009, pp. 502–513. doi:10.1016/j.ijthermalsci.2008.05.007

[15] Huang, C. H., and Chen, C. A., "A Three-Dimensional Inverse Geometry Problem in Estimating the Space and Time-Dependent Shape of an Irregular Internal Cavity," *International Journal of Heat and Mass Transfer*, Vol. 52, Nos. 7–8, 2009, pp. 2079–2091. doi:10.1016/j.ijheatmasstransfer.2008.10.024

[16] Vargas, J. V. C., and Bejan, A., "The Optimal Shape of the Interface Between Two Conductive Bodies with Minimal Thermal Resistance," *Journal of Heat Transfer*, Vol. 124, No. 6, 2002, pp. 1218–1221. doi:10.1115/1.1497355

[17] Huang, C. H., and Shih, C. C., "A Shape Identification Problem in Estimating Simultaneously Two Interfacial Configurations in a Multiple Region Domain," *Applied Thermal Engineering*, Vol. 26, No. 1, 2006, pp. 77–88. doi:10.1016/j.applthermaleng.2005.04.019

[18] Alifanov, O. M., *Inverse Heat Transfer Problem*, Springer–Verlag, Berlin, 1994.

[19] Lasdon, L. S., Mitter, S. K., and Warren, A. D., "The Conjugate Gradient Method for Optimal Control Problem," *IEEE Transactions on Automatic Control*, Vol. 12, No. 2, 1967, pp. 132–138. doi:10.1109/TAC.1967.1098538

[20] IMSL Library Edition 10.0 User's Manual: Math Library Ver. 1.0, IMSL, Houston, TX, 1987.